



## Research paper

# Fluorescence study of the effect of the oxidized phospholipids on amyloid fibril formation by the apolipoprotein A-I N-terminal fragment



Kateryna Vus<sup>a,\*</sup>, Mykhailo Grych<sup>b</sup>, Valeriya Trusova<sup>a</sup>, Galyna Gorbenko<sup>a</sup>, Paavo Kinnunen<sup>c</sup>, Chiharu Mizuguchi<sup>d</sup>, Hiroyuki Saito<sup>d</sup>

<sup>a</sup> Department of Nuclear and Medical Physics, V.N. Karazin Kharkiv National University, 4 Svobody Sq., Kharkiv 61022, Ukraine

<sup>b</sup> Department of Physics, University of Helsinki, 2a Gustaf Hällströmin katu, Helsinki FIN-00014, Finland

<sup>c</sup> Department of Neuroscience and Biomedical Engineering, School of Science and Technology, Aalto University, 3J Otakaari, Espoo FI-00076, Finland

<sup>d</sup> Department of Biophysical Chemistry, Kyoto Pharmaceutical University, 5 Nakauchi-cho, Misasagi, Yamashina-ku, Kyoto 607-8414, Japan

## ARTICLE INFO

## Article history:

Received 5 July 2017

In final form 16 September 2017

Available online 23 September 2017

## ABSTRACT

The effects of the oxidized phospholipids (oxPLs) on amyloid fibril formation by the apolipoprotein A-I variant 1-83/G26R have been investigated using Thioflavin T fluorescence assay. All types of the PoxnoPC assemblies (dispersions, micelles and lipid bilayer vesicles) induced retardation of amyloid nucleation and elongation and the enhancement of the 1-83/G26R fibrillization, although PazePC micelles completely prevented protein aggregation at low protein-to-lipid molar ratios. The ability of PazePC to inhibit 1-83/G26R aggregation was explained by the protein-lipid electrostatic interactions, which either stabilize the  $\alpha$ -helical structure of the membrane-associated 1-83/G26R or facilitate the protein solubilization by the detergent micelles.

© 2017 Elsevier B.V. All rights reserved.

## 1. Introduction

The oxidative stress is known to play a critical role in a wide variety of pathological states including the amyloid disorders, such as Alzheimer's (AD), Creutzfeldt–Jakob diseases (CJD), Parkinson's (PD), systemic amyloidosis (SA), etc. Furthermore, the damage of proteins, lipids and DNA by reactive oxygen species (ROS) precedes the appearance of a major hallmark of these pathologies, amyloid fibril formation by specific proteins: A $\beta$  peptide (AD) [1–3], prion protein (CJD) [4],  $\alpha$ -synuclein (PD) [5], lysozyme (SA) [6,7], etc.

Apolipoprotein A-I (apoA-I) is the main component of the plasma high density lipoproteins (HDL) involved in the two main processes: (i) transferring the excess of cholesterol to the liver (reverse cholesterol transport) [8]; and (ii) mediating the antioxidative processes in the low density lipoproteins (LDL) [9,10]. The HDL oxidation by myeloperoxidase in patients with established atherosclerosis has been demonstrated to limit their ability to participate in the reverse cholesterol transport [11]. Furthermore, the oxidation of methionine residues of apoA-I and genetic mutations, particularly, Iowa mutation (G26R) resulted in the amyloid fibril formation, associated with low HDL level and hereditary amyloidosis [12,13].

Protein amyloidogenesis has been proved to be a membrane-associated process, with lipid bilayer acting as a matrix which favours the aggregation-competent conformation of the polypeptide chain, interfacial accumulation and specific orientation of membrane-bound proteins [14,15]. In turn, oxidatively damaged membranes possess the extended lipid conformation, altered polarity profile, lowered energy barrier for lipid flip-flop, and at high degree of oxidation the oxPLs could form dispersions/micelles in the extracellular fluid (after the membrane damage), mediating the protein aggregation [16]. Indeed, ionic detergents have been reported to induce destabilization of the native protein structure, followed by amyloid fibril formation [17–19] presumably due to the coating of the hydrophobic surface of the proteins with the alkyl chains of the detergent molecules [20]. Therefore, of great interest in this context is the modulation of amyloid fibril formation by the oxPLs assemblies.

The assemblies of the two stable lipid oxidation products, namely 1-palmitoyl-2-azelaoyl-sn-glycero-3-phosphocholine (PazePC) and 1-palmitoyl-2-(9'-oxononanoyl)-sn-glycero-3-phosphocholine (PoxnoPC) have been recently reported to enhance the fibrillization of Temporin B and L, and gelsolin, associated with the development of the prion disease, type 2 diabetes, and hereditary amyloidosis [21,22]. According to the molecular dynamic simulations, in the lipid bilayer the polar chain of PazePC is oriented in such a manner that the carboxyl group is located in the

\* Corresponding author at: 38-12 Aeroftskaya Str., Kharkiv 61031, Ukraine.

E-mail address: [kateryna\\_vus@yahoo.com](mailto:kateryna_vus@yahoo.com) (K. Vus).

aqueous phase, while the carbonyl group of PoxnoPC resides in the glycerol backbone region [23]. This allows the Schiff-base or  $\beta$ -sheet formation between the protein and membrane surface, followed by the protein aggregation [21,22]. However, the precise mechanisms underlying such effects remain largely unknown. Furthermore, some lines of evidence suggest the complex nature of oxidative modification of the protein structure due to the recently reported inhibition of amyloid fibril formation by the oxPLs or metal oxides [24,25]. Specifically, our recent studies showed that the lipid bilayers containing PoxnoPC, triggered insulin fibrillization at physiological pH, while those containing PazePC, inhibited this process as compared to the POPC bilayers [24]. To gain deeper insight into the effects of PazePC and PoxnoPC on the protein aggregation, we further extended our investigations to the N-terminal 1-83 fragment of human apolipoprotein A-I (1-83) and its aggregation-competent variant G26R (1-83/G26R) [12]. More specifically, the present study was aimed at monitoring the kinetics of 1-83/G26R fibrillization *in vitro* using Thioflavin T assay and testing the ability of the oxPLs to inhibit the amyloid growth. Our goals were: (i) to estimate the kinetic parameters of the protein aggregation in the presence of lipids; (ii) to compare the effects of the oxPLs-containing liposomes, micelles and dispersions on 1-83 and 1-83/G26R fibrillization; (iii) to uncover the mechanism of the oxPLs-mediated amyloidogenesis of the N-terminal 1-83 fragment of apolipoprotein A-I.

## 2. Materials and methods

### 2.1. Materials

The N-terminal 1-83 fragment of human apolipoprotein A-I (1-83) and its variant G26R (1-83/G26R) were expressed and purified as described previously [12,26]. Thioflavin T was from Molecular Probes (Oregon, USA). The dye stock solution was prepared in Tris-HCl buffer (150 mM NaCl, 0.01% NaN<sub>3</sub>, pH 7.4). ThT concentration was determined spectrophotometrically using the extinction coefficient  $\epsilon_{412} = 23,800 \text{ M}^{-1} \text{ cm}^{-1}$ . 1-palmitoyl-2-azelaoyl-sn-glycero-3-phosphocholine (PazePC), 1-palmitoyl-2-(9'-oxononanoyl)-sn-glycero-3-phosphocholine (PoxnoPC), and 1-palmitoyl-2-oleoyl-sn-glycero-3-phosphocholine (POPC) lipids were from Avanti Polar Lipids (Alabaster, AL). The structures of the used lipids are shown in Fig. 1.

### 2.2. Preparation of lipid dispersions, micelles and vesicles

Lipid dispersions and vesicles were obtained as described previously [27]. Briefly, the sonication was employed to obtain lipid dispersions (below and above critical micelle concentration). The 100-nm lipid vesicles from POPC and its mixtures with PazePC (20 mol%) or PoxnoPC (20 mol%) were prepared by the extrusion technique.

### 2.3. The kinetics of amyloid formation monitored by Thioflavin T assay

The apoA-I N-terminal fragments 1-83 and 1-83/G26R were freshly dialyzed from 6 M guanidine hydrochloride solution into 10 mM Tris buffer (150 mM NaCl, 0.01% NaN<sub>3</sub>, pH 7.4) before use. The kinetics of amyloid formation by the 1-83 and 1-83/G26R fragments was monitored by Thioflavin T assay. Specifically, 96-well plates (Frickenhausen, Germany) filled with the dye (10  $\mu\text{M}$ ), proteins (5  $\mu\text{M}$ ) and lipids (0 – control samples, 0.5, 5 or 50  $\mu\text{M}$ ) were loaded into a fluorescence microplate reader (SPECTRAFluor Plus, Tecan, Austria), heated to 37 °C and incubated under constant shaking up to several days. ThT fluorescence was recorded over time at 485 nm (10 nm bandpass filter) using excitation at 430 nm (35 nm bandpass filter).

The quantitative characteristics of the fibrillization process were obtained by approximating the time ( $t$ ) dependence of ThT fluorescence intensity at 485 nm ( $F$ ) with the sigmoidal curve [12]:

$$F = F_0 + \frac{F_{\max} - F_0}{1 + \exp[k(t_m - t)]}, \quad (1)$$

where  $F_0$  and  $F_{\max}$  are ThT fluorescence intensities in the free form and in the presence of protein after the saturation has been reached, respectively;  $k$  is the apparent rate constant for the fibril growth;  $t_m$  is the time needed to reach 50% of maximal fluorescence. The lag time was calculated as:  $t_m - 2/k$ .

## 3. Results and discussion

As seen in Fig. 2, the effect of the oxidized phospholipids on the fibrillization of 1-83/G26R varies with the lipid structure and concentration. Specifically, the most pronounced (up to  $\sim 3$  times) increase in the maximum Thioflavin T fluorescence  $F_{\max}$ , which is proportional to the extent of fibril formation, was observed at

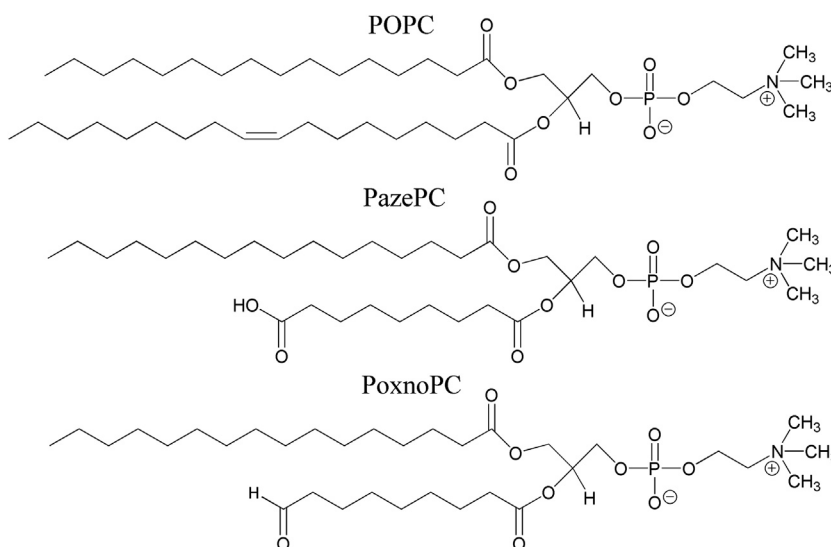
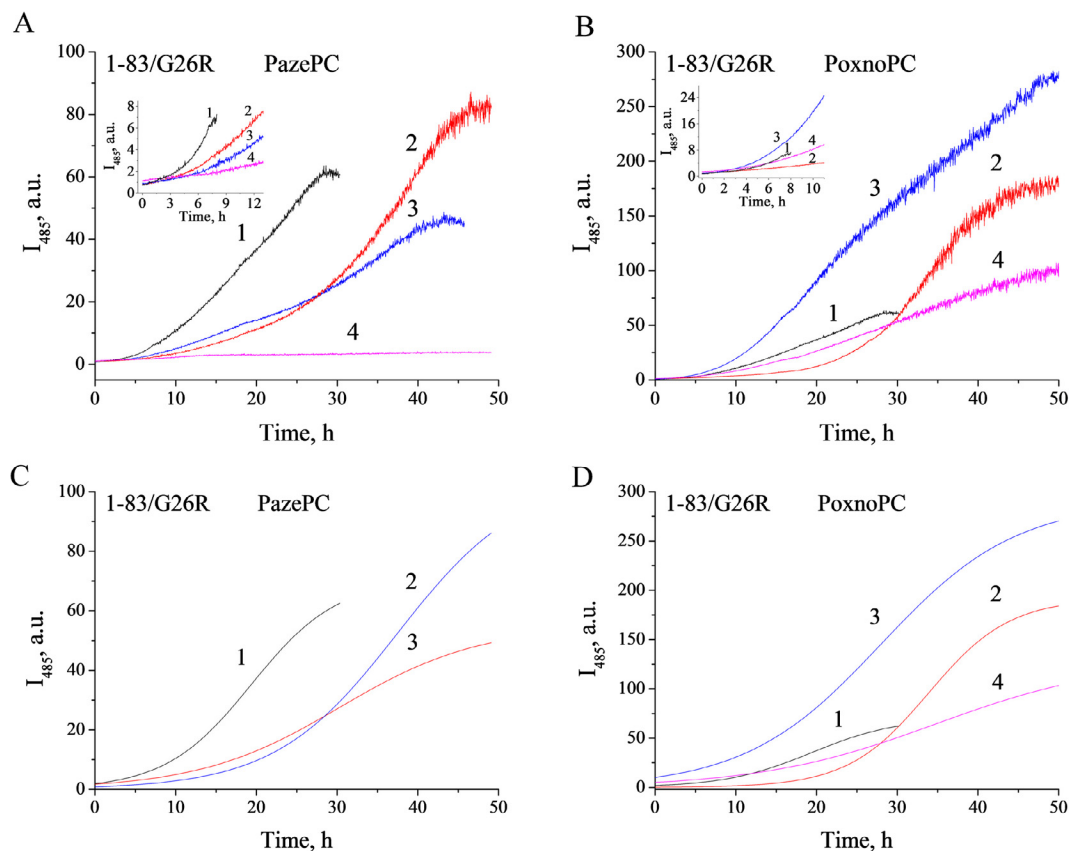


Fig. 1. Structures of 1-palmitoyl-2-oleoyl-sn-glycero-3-phosphocholine (POPC), 1-palmitoyl-2-azelaoyl-sn-glycero-3-phosphocholine (PazePC) and 1-palmitoyl-2-(9'-oxononanoyl)-sn-glycero-3-phosphocholine (PoxnoPC).



**Fig. 2.** Fibrillization kinetics of the apoA-I 1-83/G26R variant in the absence or presence of PazePC (A – experimental, C – fitted curves) and PoxnoPC (B – experimental, D – fitted curves) lipid dispersions: 1 – no lipid, 2,3,4 – correspond to protein-to-lipid molar ratios 10:1, 1:1 and 1:10, respectively. The insets show ThT fluorescence increase observed during the lag phase. Protein concentration was 5  $\mu\text{M}$ , ThT concentration was 10  $\mu\text{M}$ . PazePC and PoxnoPC concentrations were 0.5  $\mu\text{M}$ , 5  $\mu\text{M}$  and 50  $\mu\text{M}$ .

the protein-to-lipid molar ratio 1:1 (Table 1) [28]. Likewise, above the critical micelle concentration (at lipid concentration 50  $\mu\text{M}$ ), the lowest  $F_{\text{max}}$  values were recovered [29]. The fact that below the CMC (18.7 and 21.6  $\mu\text{M}$  for PazePC and PoxnoPC, respectively) Thioflavin T fluorescence was proportional to the lipid concentration, while above the CMC it substantially decreased, agrees with the results reported by Mahalka et al. for the fibrillization of gelsolin fragments, induced by PoxnoPC [29,30]. Furthermore, this tendency was also observed for the insulin fibrillization in the presence of PazePC [24]. Notably, the opposite effects of the PoxnoPC and PazePC on the 1-83/G26R aggregation at the lipid concentrations 5  $\mu\text{M}$  and 50  $\mu\text{M}$  could be attributed to the different

mechanisms of the protein interaction with lipid dispersions and micelles [27].

Next, both oxPLs slowed down the 1-83/G26R nucleation, resulting in a substantial increase in the lag time (up to 3-fold) and decrease in the fibrillization rate  $k$  (up to 5-fold), as compared to the control samples (Table 1). Similarly, the extension of the lag time was observed for FtG<sub>179–194</sub> gelsolin fragment in the presence of PoxnoPC [30].

Furthermore, at the protein-to-lipid molar ratio 1:1, PazePC induced less pronounced enhancement of the 1-83/G26R fibrillization than PoxnoPC. The former also exerted inhibiting effect on the protein fibrillization at the smaller or greater protein-to-lipid

**Table 1**  
Kinetic parameters of amyloid formation by apoA-I 1-83 and apoA-I 1-83/G26R in the presence of oxidized phospholipids.

System	$F_{\text{max}}$ , a.u.	$t_m$ , h	$k \cdot 10^{-3}$ , h <sup>-1</sup>	Lag time, h	$R^2$
1-83	132.6 ± 1.5	89.5 ± 0.1	28.5 ± 0.2	18.8 ± 0.1	0.995
1-83 + PazePC (1:10)	– <sup>a</sup>	–	–	–	–
1-83 + PoxnoPC (1:10)	54.3 ± 0.2	176.2 ± 1.7	15.2 ± 0.1	44.6 ± 1.7	0.994
1-83/G26R	70.5 ± 0.3	19.5 ± 0.1	188 ± 1	8.9 ± 0.1	0.997
1-83/G26R + PazePC (1:10)	– <sup>a</sup>	–	–	–	–
1-83/G26R + PazePC (1:1)	105.3 ± 1.1	37.5 ± 0.0	131 ± 0	22.2 ± 0.0	0.997
1-83/G26R + PazePC (10:1)	55.1 ± 0.4	30.3 ± 0.0	114.5 ± 0.4	12.8 ± 0.0	0.994
1-83/G26R + PoxnoPC (1:10)	129 ± 1.4	35.1 ± 0.2	92.4 ± 0.7	13.5 ± 0.2	0.994
1-83/G26R + PoxnoPC (1:1)	290 ± 2.8	28.3 ± 0.2	119.0 ± 1.5	11.5 ± 0.2	0.992
1-83/G26R + PoxnoPC (10:1)	191 ± 1.6	34.0 ± 0.2	200 ± 2	24.0 ± 0.2	0.997
1-83/G26R + POPC	155.8 ± 0.4	132.0 ± 0.0	53.2 ± 0.0	94.4 ± 0.0	0.999
1-83/G26R + POPC/PazePC (20 mol%)	109.8 ± 0.05	124.7 ± 0.1	36.3 ± 0.1	69.6 ± 0.1	0.999
1-83/G26R + POPC/PoxnoPC (20 mol%)	158.3 ± 0.05	125.5 ± 0.0	41.5 ± 0.1	77.3 ± 0.0	0.999

<sup>a</sup> No Thioflavin T fluorescence response was observed for the systems 1-83 + PazePC (1:10) and 1-83/G26R + PazePC (1:10).

molar ratios (Table 1). Specifically, no change in ThT fluorescence was observed upon the 1-83/G26R incubation in the presence of 50  $\mu\text{M}$  PazePC, indicating that lipid micelles prevent the protein fibrillization. Similarly, Mahalka et al. demonstrated that PazePC did not have a noticeable influence on the fibrillization of FtG<sub>179–194</sub> gelsolin fragment, while PoxnoPC promoted the peptide aggregation [30]. In turn, PazePC enhanced the fibrillization of lysozyme and insulin, showing a more significant effect on the insulin aggregation than PoxnoPC [24]. The latter may result from the specific interactions of the carboxyl group of PazePC with insulin, inducing its partial denaturation and transition into the aggregation-prone conformation [24].

As seen in Fig. 3, the lag time of amyloid fibril formation by 1-83/G26R in the absence of lipids was about 3 times smaller, and the fibrillization rate was 6 times greater, as compared to the correspondent values for the 1-83 aggregation. These results are in harmony with the data of Adachi et al., suggesting that G26R mutation enhanced the amyloid fibril formation [11]. Furthermore, the apparent rate constant for the 1-83 fibril growth in the presence of the oxPLs was twice than its control value, the lag time was increased 2-fold, and the fibrillization extent was reduced (Table 1). Thus, similarly to the 1-83/G26R, the 1-83 forms a smaller number of fibrils in the presence of PazePC micelles.

In the following, the effect of lipid vesicles composed of POPC and its mixtures with the oxPLs on the 1-83/G26R amyloid fibril formation has been evaluated. As seen in Fig. 4 and Table 1, the addition of liposomes to the protein solution induced  $\sim 2$ -fold increase of the  $F_{\text{max}}$ ,  $\sim 3$ – $5$ -fold decrease of the  $k$  value, and  $\sim 9$ – $12$ -fold extension of the lag time. This tendency is in good agreement with the previously reported data obtained for FtG<sub>179–194</sub> gelsolin fragment and insulin [24,30]. Specifically, PoxnoPC and PazePC incorporated into the liposomal membranes slowed down the kinetics of amyloid fibril formation, as compared to the control samples and lipid dispersions [24,30].

Furthermore, the effects of POPC, POPC/PazePC (20 mol%) and POPC/PoxnoPC (20 mol%) on the 1-83/G26R aggregation did not vary significantly, although inclusion of PazePC into POPC bilayer resulted in the  $\sim 40\%$  decrease in the fibrillization extent, as compared to the neat POPC liposomes (Table 1). Notably, the fact that PazePC micelles prevented amyloid fibril formation by the apoA-I amyloidogenic fragment at the low lipid-to-protein weight ratio  $\sim 0.8$  (Fig. 2), while POPC/PazePC (20 mol%) liposomes slowed down the kinetics of the protein aggregation (Fig. 4), suggest that the observed effects are governed by specific PazePC-1-83/G26R interactions with the lipid bilayers or micelles. These results,

together with those reported for FtG<sub>179–194</sub> gelsolin fragment, highlight a critical role of PazePC in inhibiting the amyloid fibril formation by the short (unstructured) peptides [30], although this lipid seems to induce misfolding and aggregation of the full-length proteins, like lysozyme or insulin, more effectively than PoxnoPC [24]. Interestingly, the oxPLs have been found to accelerate the amyloid nucleation, presumably due to the perturbation of the membrane structure and dynamics by the oxidized lipid tails [31].

Recently, Saito et al. have reported the enhancement of the 1-83/G26R aggregation on POPC membranes produced by the G26R amyloidogenic mutation [28]. In contrast, no ThT fluorescence response was observed in the case of 1-83 at the lipid-to-protein weight ratio  $\sim 30$ . Our study indicates that the 1-83/G26R still retains the ability to form amyloid fibrils in the presence of vesicles containing the oxPLs at the lipid-to-protein weight ratio  $\sim 31$  (Fig. 4). It can be assumed that there exist the  $\alpha$ -helices formed by the unstructured 1-83/G26R on the membrane surface, which are destabilized regardless of the presence of PazePC [11,28]. Such a destabilization induced by the G26R mutation promotes further transformation of the helices into the  $\beta$ -sheets, followed by the amyloid fibril formation on the membrane surface, being a common mechanism for the natively unstructured proteins and peptides involved in amyloid pathologies [32,33].

Interestingly, the properties of the complexes formed by the apoA-I variants with phosphatidylcholine vesicles have been characterized previously, reporting also the binding parameters for 1-83 and 1-83/G26R [28]. Using these parameters, we found that at the lipid concentration 2 mM and protein concentration 5  $\mu\text{M}$  the fraction of bound protein is  $\sim 90\%$  for 1-83 and  $\sim 65\%$  for 1-83/G26R. But the point is that the formation of the protein-lipid complexes and ThT complexes with monomeric protein or lipids occurs in the time scale much faster than that characteristic of fibril growth and the equilibrium is attained within the first hour of the incubation of the protein-lipid-dye mixture. Likewise, the complexation of ThT with the protein oligomers formed during the lag phase is not followed by sigmoidal fluorescence increase specific for fibrillar aggregates [34–36]. Therefore, we are prone to think that the kinetic curves presented here reflect the formation of fibrillar aggregates, while the weak fluorescence increase observed during the lag phase (shown in insets in Figs. 2A, B, 4A) characterizes the dye association with fibril intermediates. Similarly, we did not determine the fraction of the protein bound to pre- or micellar aggregates, because within the employed experimental conditions the transient protein aggregates are formed and the equilibria between various types of complexes are continuously shifting.

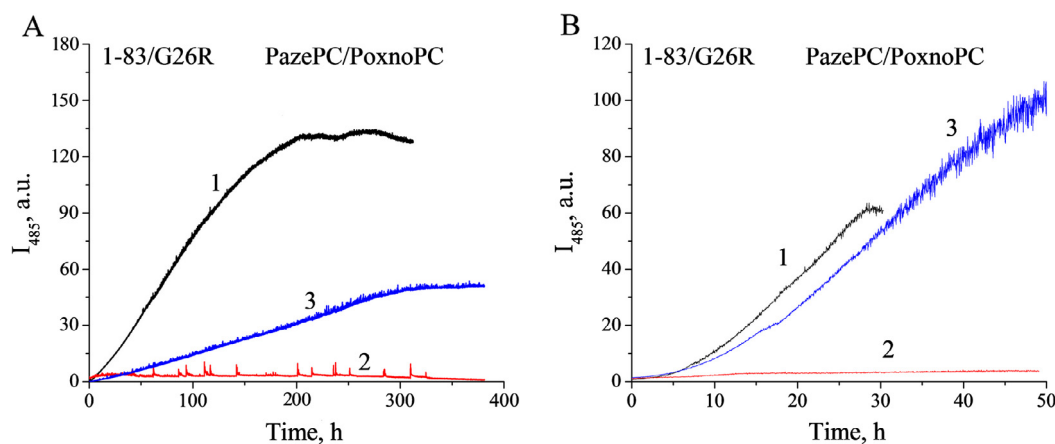


**Fig. 3.** Fibrillization kinetics of the apoA-I 1-83 (A) and 1-83/G26R (B) variants in the absence or presence of PazePC and PoxnoPC lipid dispersions: 1 – no lipid, 2 – PazePC, 3 – PoxnoPC. Protein concentration was 5  $\mu\text{M}$ , ThT concentration was 10  $\mu\text{M}$ . PazePC and PoxnoPC concentrations were 50  $\mu\text{M}$ , corresponding to the protein-to-lipid molar ratio 1:10.

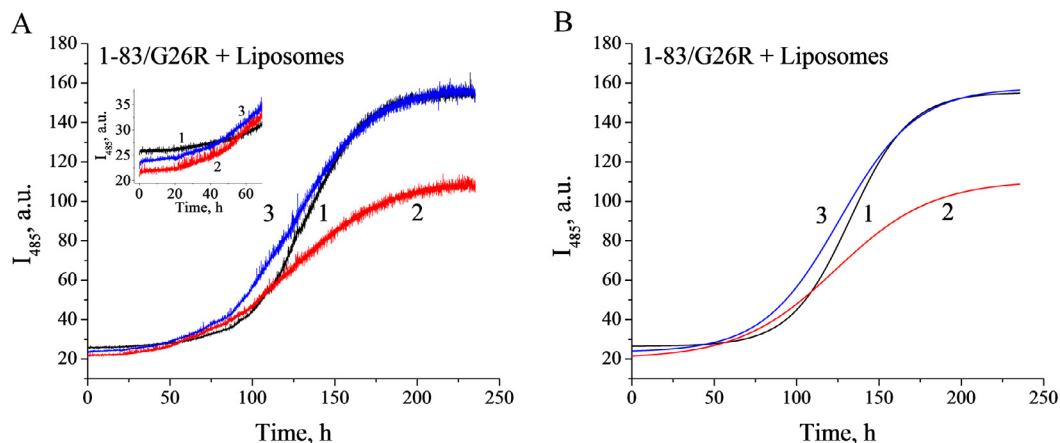


**Fig. 4.** Fibrillization kinetics of the apoA-I 1-83/G26R variant in the presence of: 1 – POPC, 2 – POPC/PazePC (20 mol%), 3 – POPC/PoxnoPC (20 mol%) liposomes (A – experimental, B – fitted curves). Protein concentration was 5  $\mu$ M, ThT concentration was 10  $\mu$ M. The insets show ThT fluorescence increase observed during the lag phase. Lipid concentration was 2 mM, corresponding to POPC-to-apoA-I weight ratio  $\sim$ 31.

In order to clarify the mechanism of the oxPLs-mediated 1-83/G26R fibril formation, the number of micelles and the protein-to-micelle ratios have been estimated. Lipid concentration of the micellar phase and total surface area of one micelle have been estimated using the CMC values and previously reported thicknesses of the pure POPC and PazePC-containing bilayers [37–39]. The obtained surface area was ca.  $\sim$ 41.6 nm<sup>2</sup>, corresponding to  $\sim$ 47.4 lipid molecules in one roughly spherical micelle [40,41]. Finally, protein-to-micelle molar ratios were calculated to be ca.  $\sim$ 7.6 and  $\sim$ 8.3 for PazePC and PoxnoPC, respectively.

Similarly to the cationic protein cytochrome *c*, the arginine and lysine residues of 1-83/G26R could electrostatically attach to the outer surface of PazePC micelles, resulting in a better solubilization of the protein (Fig. 5) [41]. Next, protein-solubilized micelles can undergo the transformation into tubular structures by fusion, coating the nonpolar face of the protein and allowing the transition to a stable  $\alpha$ -helical conformation [42,43]. Accordingly, the proteomicelles will be composed of the tubular PazePC micelle (radius  $\sim$ 1.8 nm, height  $\sim$ 5 nm, comparable with the dimensions of the membrane-bound 1-83 [44]), surrounded by up to 8 1-83/G26R molecules. The proteomicelle formation may reduce the concentration of aggregation-prone 1-83/G26R. Alternatively, 1-83/G26R does not adsorb on the micelle surface, but similarly to the membrane proteins, interacts with PazePC monomers by electrostatic and hydrophobic interactions, resulting in the formation of the lipid monolayer, covering the hydrophobic surface of the protein and reducing the apparent CMC [20,45,46]. Interestingly, polar interactions between the charged amino acids and phosphatidylcholine headgroups could also favor the formation of the neat

detergent micelle that may result in the decrease of the apparent CMC [20]. Lipid binding to the natively unfolded 1-83/G26R is unlikely to alter the protein secondary structure, although lipid embedding into the amyloid nucleus may occur above/below the CMC [17,30]. In turn, 1-83G26R binding to PoxnoPC micelles is weaker presumably due to the lack of the lipid-protein covalent interactions, resulting in the fibrillization of the free protein in buffer (Fig. 2B) [41]. Furthermore, Schiff base formation between 1-83/G26R and PoxnoPC dispersions, adsorbed on the hydrophobic protein surface, could induce the protein cross-linking and lipid embedding into the oligomers and amyloid fibrils [20,30,45]. The suggested mechanisms may lead to the lag time increase and the decrease/increase in the 1-83/G26R aggregation extent depending on the PazePC/PoxnoPC concentration (Table 1).

Finally, in order to explain the decrease of the 1-83/G26R fibrillization extent induced by the POPC/PazePC (20 mol%) vesicles/micelles, a graphical model for the association between the 1-83/G26R and POPC/PazePC bilayer has been suggested (Fig. 5). According to this model, the nonpolar faces of the amphipathic helices of the ApoA-I N-terminal fragment, interact with the lipid bilayer while their polar faces are in contact with the aqueous phase [47,48]. The two panels in Fig. 5 are the helical wheel projections of the residues 8–27 and 36–65, containing the most aggregation-prone regions 14–22 and 49–57 [28]. Obviously, the positively charged amino acid residues of the ApoA-I N-terminal fragment could associate with the *sn*-2 chain of PazePC extended into the aqueous phase via strong electrostatic interactions [23,31]. This may increase free energy of denaturation of the  $\alpha$ -helices and, as a consequence, reduce the fibrillization extent,

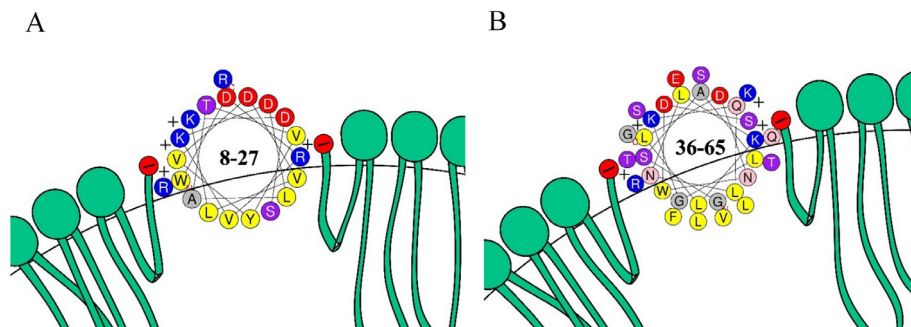


**Fig. 5.** Schematic illustration of the model for the association between 1-83/G26R and POPC/PazePC (20 mol%) bilayer. The black line represents the hydrophilic-hydrophobic interface of the bilayer leaflet.

as compared to the neat POPC vesicles. Notably, it is PazePC interaction with the residue R26 that could be critical for the inhibition of the 1-83/G26R aggregation by the oxidized phospholipids [28]. Interestingly, surface area of one liposome with the diameter *ca.* 100 nm was *ca.*  $\sim 6 \cdot 10^4 \text{ nm}^2$  [40,49]. Accordingly, the calculated protein-to-liposome molar ratio was  $\sim 232$  for the POPC and  $\sim 218$  for the oxPLs-containing lipid vesicles, respectively. Furthermore, significant increase in the lag time of the 1-83/G26R fibril formation in the presence of the lipid vesicles seems to result from the above effect [28].

#### 4. Conclusions

In conclusion, our fluorescence studies demonstrated that the kinetic parameters of the 1-83/G26R fibrillization vary significantly with the oxPLs structure, the concentration and the type of lipid assemblies (dispersions, micelles or lipid bilayer vesicles). Specifically, membrane/micelle surfaces were found to play a critical role in the inhibition of the amyloid fibril formation, presumably due to their ability to stabilize  $\alpha$ -helical structure of the 1-83/G26R or facilitate the protein solubilization by the protein-lipid electrostatic and covalent interactions. Furthermore, the increase in the lag time of the 1-83/G26R fibrillization induced by the oxPLs suggests that their binding to the protein hampered the formation of amyloid nuclei. Overall, the effects of oxidized lipids revealed in the present study may prove useful in the development of anti-amyloid strategies.

#### Acknowledgements

This work was supported by the Ministry of Education and Science of Ukraine (the Young Scientist project 'Design of the novel methods of fluorescence diagnostics of amyloid pathologies', project number: 0116U000937).

#### References

- [1] P. Poprac, K. Jomova, M. Simunkova, V. Kollar, C.J. Rhodes, M. Valko, *Trends Pharmacol. Sci.* 38 (2017) 592.
- [2] T. Jiang, Q. Sun, S. Chen, *Prog. Neurobiol.* 147 (2016) 1.
- [3] D.J. Bonda, H. Lee, J.A. Blair, X. Zhu, G. Perry, M.A. Smith, *Metalomics* 3 (2011) 267.
- [4] S. Chen, S. He, J.K. Shang, M.M. Ma, C.S. Xu, X.H. Shi, J.W. Zhang, *Clin. Biochem.* 49 (2016) 292.
- [5] G.B. Irvine, O.M. El-Agnaf, G.M. Shankar, D.M. Walsh, *Mol. Med.* 14 (2008) 451.
- [6] S. Ghosh, N.K. Pandeya, S. Bhattacharya, A. Roy, N.V. Nagyc, S. Dasgupta, *Int. J. Biol. Macromol.* 76 (2015) 1.
- [7] M.S. Petrônio, V.F. Ximenes, *Biochim. Biophys. Acta* 1824 (2012) 1090.
- [8] A.R. Tall, *J. Int. Med.* 263 (2008) 256.
- [9] A. Kontush, S. Chantepie, M.J. Chapman, *Arterioscl., Thrombosis, Vas. Biol.* 23 (2003) 1881.
- [10] M. Navab, S.Y. Hama, C.J. Cooke, G.M. Anantharamaiah, M. Chaddha, L. Jin, G. Subbanagounder, K.F. Faull, S.T. Reddy, N.E. Miller, A.M. Fogelman, *J. Lipid Res.* 41 (2000) 1481.
- [11] E. Adachi, H. Nakajima, C. Mizuguchi, P. Dhanasekaran, H. Kawashima, K. Nagao, K. Akaji, S. Lund-Katz, M.C. Phillips, H. Saito, *J. Biol. Chem.* 288 (2013) 2848.
- [12] B. Shao, G. Cavignolo, N. Brot, M.N. Oda, J.W. Heinecke, *Proc. Natl. Acad. Sci. U.S.A.* 105 (2008) 12224.
- [13] N.A. Ramella, G.R. Schinella, S.T. Ferreira, E.D. Prieto, M.E. Vela, J.L. Rios, M.A. Tricerri, O.J. Rimoldi, *PLoS One* 7 (2012) e43755.
- [14] M. Stefani, *Int. J. Mol. Sci.* 9 (2008) 2515.
- [15] C. Aisenbrey, T. Borowik, R. Byström, M. Bokvist, F. Lindström, H. Misiak, M.-A. Sani, G. Gröbner, *Europ. Biophys. J.* 37 (2008) 247.
- [16] R. Volinsky, L. Cwiklik, P. Jurkiewicz, M. Hof, P. Jungwirth, P.K.J. Kinnunen, *Biophys. J.* 101 (2011) 1376.
- [17] Z. Yang, C. Wang, Q. Zhou, J. An, E. Hildebrandt, L.A. Aleksandrov, J.C. Kappes, L. J. DeLucas, J.R. Riordan, I.L. Urbatsch, J.F. Hunt, G.G. Brouillette, *Protein Sci.* 23 (2014) 769.
- [18] J.V. Møller, M. le Maire, *J. Biol. Chem.* 268 (1993) 18659.
- [19] V.N. Uversky, M. Cooper, K.S. Bower, J. Li, A.L. Fink, *FEBS Lett.* 515 (2002) 99.
- [20] R.A. Böckmann, A. Caffisch, *Biophys. J.* 88 (2005) 3191.
- [21] A.K. Mahalka, P.K.J. Kinnunen, *Biochim. Biophys. Acta* 1788 (2009) 600.
- [22] P.K. Kinnunen, K. Kaarniranta, A.K. Mahalka, *Biochim. Biophys. Acta* 1818 (2012) 2446.
- [23] H. Khandelia, O.G. Mouritsen, *Biophys. J.* 96 (2009) 2734.
- [24] K. Vus, R. Sood, G. Gorbenko, P. Kinnunen, *Methods Appl. Fluoresc.* 4 (2016) 034008.
- [25] A. Bellova, E. Bystrenova, M. Koneracka, P. Kopcansky, F. Valle, N. Tomasovicova, M. Timko, J. Bagelova, F. Biscarini, Z. Gazova, *Nanotechnology* 21 (2010) 065103.
- [26] M. Girysh, G. Gorbenko, V. Trusova, E. Adachi, C. Mizuguchi, K. Nagao, H. Kawashima, K. Akaji, S. Lund-Katz, M.C. Phillips, H. Saito, *J. Struct. Biol.* 185 (2014) 116.
- [27] N.-J. Cho, L.Y. Hwang, J.J.R. Solandt, C.W. Frank, *Materials* 6 (2013) 3294.
- [28] C. Mizuguchi, F. Ogata, S. Mikawa, K. Tsuji, T. Baba, A. Shigenaga, T. Shimanouchi, K. Okuhira, A. Otaka, H. Saito, *J. Biol. Chem.* 290 (2015) 20947.
- [29] J.-P. Mattila, K. Sabatini, P.K.J. Kinnunen, *Biophys. J.* 93 (2007) 3105.
- [30] A.K. Mahalka, C.P.J. Maury, P.K.J. Kinnunen, *Biochemistry* 50 (2011) 4877.
- [31] R. Volinsky, P.K. Kinnunen, *FEBS J.* 280 (2013) 2806.
- [32] G.P. Gorbenko, P.K. Kinnunen, *Chem. Phys. Lipids.* 141 (2006) 72.
- [33] E.R. Georgieva, T.F. Ramlall, P.P. Borbat, J.H. Freed, D. Eliezer, *J. Biol. Chem.* 285 (2010) 28261.
- [34] H. Naiki, K. Higuchi, M. Hosokawa, T. Takeda, *Anal. Biochem.* 177 (1989) 244.
- [35] H. LeVine III, *Protein Sci.* 2 (1993) 404.
- [36] A.A. Maskevich, V.I. Stsiapura, V.A. Kuzmitsky, I.M. Kuznetsova, O.I. Povarova, V.N. Uversky, K.K. Turoverov, *J. Proteome Res.* 6 (2007) 1392.
- [37] C.R. Cantor, P.R. Schimmel, *Biophysical Chemistry: Part III: The Behavior of Biological Macromolecules*, first ed., WH Freeman, San Francisco, 1980, 524 P.
- [38] F.T. Mendes, R. Sood, R. Bärenwald, G. Carlström, D. Topgaard, K. Saalwächter, P.K. Kinnunen, O.H. Öllila, *Langmuir* 32 (2016) 6524.
- [39] N. Kučerka, M.P. Nieh, J. Katsaras, *Biochim. Biophys. Acta* 1808 (2011) 2761.
- [40] R. Volinsky, R. Paananen, P.K. Kinnunen, *Biophys. J.* 103 (2012) 247.
- [41] J.P. Mattila, K. Sabatini, P.K. Kinnunen, *Langmuir* 24 (2008) 4157.
- [42] M. Bourrell, R.S. Schechter, *Macroemulsions and related systems, in: Formulation, Solvency and Physical Properties*, Editions Technip, Paris, 2010, 396 P.
- [43] R. Pool, P.G. Bolhuis, *J. Chem. Phys.* 126 (2007) 244703.
- [44] X. Mei, D. Atkinson, *J. Biol. Chem.* 286 (2011) 38570.
- [45] V. Chaptal, F. Delolme, A. Kilburg, S. Magnard, C. Montigny, M. Picard, C. Prier, L. Monticelli, O. Bornert, M. Agez, S. Ravaut, C. Orelle, R. Wagner, A. Jawhari, I. Broutin, E. Pebay-Peyroula, J.M. Jault, H.R. Kaback, M. le Maire, P. Falson, *Sci Rep.* 7 (2017) 41751.
- [46] Jörg H. (Ed.), *Lipid-Protein Interactions Methods and Protocols*, Kleinschmidt, 2013, 455 P.
- [47] W.S. Davidson, T.B. Thompson, *J. Biol. Chem.* 282 (2007) 22249.
- [48] C.G. Brouillette, G.M. Anantharamaiah, J.A. Engler, D.W. Borhani, *Biochim. Biophys. Acta* 1531 (2001) 4.
- [49] G. Lantzsch, H. Binder, *J. Fluoresc.* 4 (1994) 339.